Acta Crystallographica Section F
Structural Biology and Crystallization Communications
ISSN 1744-3091

Crystallization and preliminary X-ray analysis of the oxygenase component (HpaB) of 4-hydroxyphenylacetate 3-monooxygenase from *Thermus thermophilus* HB8

Seong-Hoon Kim,[a] Hideyuki Miyatake,[a] Tamao Hisano,[a] Wakana Iwasaki,[a] Akio Ebihara[a] and Kunio Miki[a,b]*

[a]RIKEN SPring-8 Center, Koto 1-1-1, Mikazuki-cho, Sayo-gun, Hyogo 679-5148, Japan, and [b]Department of Chemistry, Graduate School of Science, Kyoto University, Sakyo-ku, Kyoto 606-8502, Japan

Correspondence e-mail: miki@kuchem.kyoto-u.ac.jp

Received 2 February 2007
Accepted 22 May 2007

The 4-hydroxyphenylacetate (4HPA) 3-monooxygenase enzyme catalyzes the hydroxylation of 4HPA to 3,4-dihydroxyphenylacetate in the initial step of the degradation pathway of 4HPA. This enzyme consists of two components: an oxygenase (HpaB) and a reductase (HpaC). HpaB hydroxylates 4HPA using an oxygen molecule and a reduced flavin, which is supplied by HpaC. HpaB from *Thermus thermophilus* HB8 was overexpressed in *Escherichia coli* and crystallized. Crystals of HpaB were grown in 0.4 *M* 1,6-hexanediol, 0.1 *M* sodium acetate pH 5.0 and 25%(*v*/*v*) glycerol and diffracted X-rays to a resolution of 1.60 Å. The crystals belong to the orthorhombic space group *I*222, with unit-cell parameters a = 91.8, b = 99.6, c = 131.1 Å. The asymmetric unit volume provides space for only one subunit of the tetrameric HpaB molecule, giving a Matthews coefficient V_M of 2.8 Å^3 Da^{-1} and a solvent content of 55.1%. Platinum-derivatized crystals of HpaB were prepared by soaking native crystals in a solution containing 1 m*M* ammonium tetrachloroplatinate(II) for 1 d and diffracted X-rays to a resolution of 2.50 Å. MAD data were successfully collected for structural determination using these crystals.

1. Introduction

The 4-hydroxyphenylacetate (4HPA) 3-monooxygenase enzyme catalyzes the hydroxylation of 4-HPA to 3,4-dihydroxyphenylacetate (DHPA) in the initial step of the degradation pathway of 4-HPA. 4HPA 3-monooxygenase consists of an oxygenase HpaB and a reductase HpaC (Cooper & Skinner, 1980; Prieto & García, 1994; Prieto *et al.*, 1996; Galán *et al.*, 2001) and is classified into the two-component flavin-diffusible monooxygenase (TC-FDM) family (Galán *et al.*, 2000). HpaB hydroxylates 4HPA using molecular oxygen and reduced flavin and HpaC reduces the resultant oxidized flavin using NAD(P)H (Fig. 1). The activity of HpaB is absolutely dependent on the presence of HpaC, but no physical interaction between the two components is required, indicating that flavins link HpaB and HpaC by free diffusion (Galán *et al.*, 2000).

The catalytic mechanisms of enzymatic hydroxylation of aromatic compounds have been extensively studied for single-component

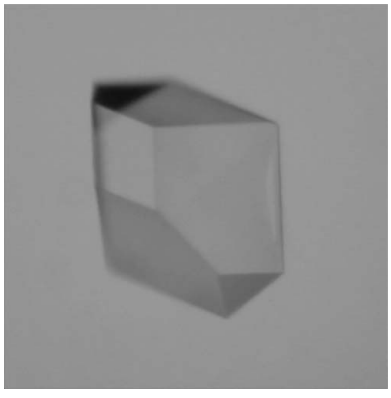

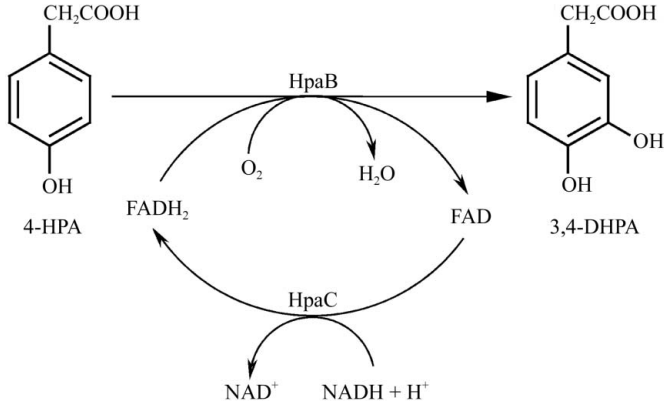

Figure 1
Reaction catalyzed by HpaB and HpaC. HpaC is an NADH:flavin reductase that supplies reduced flavin to HpaB.

enzymes such as phenol hydroxylase from *Trichosporon cutaneum* (Maeda-Yorita & Massey, 1993) and *p*-hydroxybenzoate hydroxylase from *Pseudomonas fluorescens* (van Berkel *et al.*, 1992) and *Pseudomonas aeruginosa* (Entsch *et al.*, 1975) on the basis of their crystal structures. There are remarkable differences between single- and two-component systems in their enzymatic action. Both systems include enzyme-C4a-hydroperoxyflavin intermediates during catalysis. In phenol hydroxylase and *p*-hydroxybenzoate hydroxylase, substrates are bound to the active site before the formation of the C4a-hydroperoxyflavin intermediate, so that hydroxylation of the substrate immediately occurs upon formation of the C4a-hydroperoxyflavin intermediate (Entsch *et al.*, 2005; Ballou *et al.*, 2005, and references therein). In contrast, in two-component systems substrate is bound to the active site after formation of the C4a-hydroperoxyflavin intermediate (Xun & Sandvik, 2000; Gisi & Xun, 2003; Sucharitakul *et al.*, 2006; Valton *et al.*, 2006). Thus, there must be a mechanism to stabilize unstable C4a-hydroperoxyflavin species in oxygenases of the two-component system. In addition, flavin is not a prosthetic group in HpaB and other enzymes belonging to the TC-FDM family and there must be a mechanism for binding and releasing flavin in these enzymes. A *BLAST* search suggests that 4-hydroxybutyryl-CoA dehydratase from *Clostridium aminobutyricum* (4-BUDH; PDB code 1u8v) is the closest homologue (24% sequence identity) of known structure. Interestingly, 4-BUDH, which catalyzes an oxygen-sensitive dehydration of 4-hydroxybutylryl-CoA, differs from HpaB in function. To gain insight into these interesting observations, we have initiated crystallographic studies of HpaB (481 amino acids). Here, we describe the crystallization and preliminary X-ray diffraction analysis of HpaB from *Thermus thermophilus* HB8.

2. Materials and methods

2.1. Purification of HpaB

The ORF of *hpaB* was amplified by PCR using *T. thermophilus* HB8 genomic DNA as a template and oligonucleotide primers with artificial *Nde*I and *Bgl*II sites (bold): 5′-ATAT**CATATG**GCTAGGACCGGAGCGGAGTACATCGAGG-3′ and 5′-ATAT**AGATCT**TTATTACGCCTGGACCTCCTCAAAGACCTTG-3′. The PCR product was digested with *Nde*I and *Bam*HI and was ligated into the pET11a expression plasmid (Novagen), in which the *hpaB* gene is under control of the T7 promoter. Cells were grown at 310 K in Luria–Bertani medium containing 50 µg ml^{-1} ampicillin. Culture growth continued for 24 h in *Escherichia coli* BL21 (DE3). Target protein with the chain length of the intact polypeptide was produced without IPTG induction, which is probably the consequence of an expression leak in the host strain. Cells were harvested by centrifugation at 2000*g* for 10 min at 277 K and the cell pellets were resuspended in lysis buffer (50 m*M* NaCl, 20 m*M* Tris–HCl pH 8.0, 5 m*M* 2-mercaptoethanol) and disrupted by sonication. The cell lysates were clarified by centrifugation at 200 000*g* for 60 min at 277 K. The supernatant was heated at 343 K for 10 min in order to precipitate labile *E. coli* host proteins and was centrifuged at 65 300*g* for 60 min. The supernatant was loaded onto a 6 ml Resource ISO column (Amersham Bioscience) equilibrated with 50 m*M* sodium phosphate buffer pH 7.0 containing 1.5 *M* ammonium sulfate and eluted with a linear gradient to 0 *M* ammonium sulfate. The fractions containing HpaB were eluted with 0.4 *M* ammonium sulfate. The protein pellets were dissolved in 20 m*M* Tris–HCl buffer pH 8.0. This solution was desalted using a HiPrep 26/10 desalting column (Amersham Bioscience) and applied onto a 6 ml Resource Q column (Amersham Bioscience) equilibrated with 20 m*M* Tris–HCl buffer pH 8.0. HpaB was eluted with a linear gradient of NaCl. Fractions containing HpaB were pooled and concentrated by ultrafiltration. The concentrated solution was further separated on a HiLoad 16/60 Superdex 75 pg column (Amersham Bioscience) equilibrated with 20 m*M* Tris–HCl pH 8.0 containing 150 m*M* NaCl. The fractions containing HpaB were desalted using a HiPrep 26/10 desalting column and concentrated to 12.5 mg ml^{-1} by ultrafiltration in solutions of 20 m*M* Tris–HCl buffer pH 8.0 containing 1 m*M* dithiothreitol. The protein concentration was determined by absorption measurement with a calculated molar absorption coefficient (ε_{280} = 65 625, which was obtained from the sum of the ε_{280} values for the 25 tyrosine and five tryptophan residues of HpaB). The purity of the resulting sample was confirmed by SDS–PAGE using a 12.5% separation gel and the gels were stained with Coomassie Brilliant Blue (CBB).

2.2. Crystallization

Crystallization was performed using the hanging-drop vapour-diffusion method. The protein solution was allowed to equilibrate against 500 µl reservoir solution at 293 K. Each droplet was prepared by mixing equal volumes (2–5 µl) of protein solution and reservoir solution. Crystallization was initially carried out using Crystal Screen and Crystal Screen II (Hampton Research) and the Sigma Cryo kit (Sigma). After initial crystallization trials using these screening kits, the chosen crystallization conditions were optimized by employing finer intervals of pH and precipitant concentration.

2.3. Preparation of derivative crystals

More than 50 heavy-atom compounds were surveyed for preparation of crystals of heavy-atom derivatives of HpaB. The crystals were soaked in reservoir solutions containing 1–2 m*M* of each heavy-atom compound for 1 d. A back-soaking procedure was employed for 1 min prior to data collection.

2.4. X-ray data collection

Diffraction data were collected using a Rigaku R-AXIS V imaging-plate detector on the BL45XU beamline (Kumasaka *et al.*, 2002) at SPring-8, Harima, Japan. A crystal was flash-frozen in a nitrogen-gas stream at 100 K directly from a drop containing 25%(*v*/*v*) glycerol as a cryoprotectant and was maintained at 100 K during data collection. The oscillation range used was 1.0° and the crystal-to-detector distance was set at 150 mm. The wavelength was set to 0.9000 Å for a native crystal of HpaB. MAD data were collected by the trichromatic method (Kumasaka *et al.*, 2002) using a Pt-derivatized crystal. Three wavelengths were selected by inspecting the X-ray absorption spectrum of the Pt atom in the derivative crystal, with remote, peak and edge wavelengths set for the first, second and third pairs of the trichromator, respectively, during data collection. The oscillation range used was 1.0° and the crystal-to-detector distance was set at 150 mm.

The diffraction data were processed using the *HKL*-2000 program package (Otwinowski & Minor, 1997). For the derivative data, anomalous pairs were treated as non-equivalent reflections and were kept separate during scaling using the 'SCALE ANOMALOUS' flag in the *SCALEPACK* program in *HKL*-2000 (Otwinowski & Minor, 1997).

3. Results and discussion

3.1. Crystals of HpaB

Crystals of HpaB were initially grown at 277 and 293 K under condition No. 11 of Crystal Screen II (1.0 *M* 1,6-hexanediol, 0.1 *M* sodium acetate pH 4.6, 0.01 *M* cobalt chloride). After numerous trials to optimize the crystallization conditions, crystals of X-ray quality were obtained at 293 K using a solution containing 0.4 *M* 1,6-hexanediol, 0.1 *M* sodium acetate pH 5.0 and 25%(*v*/*v*) glycerol. Crystals appeared within a few minutes and reached final dimensions of 0.25 × 0.4 × 0.2 mm after 1–3 d (Fig. 2). They diffracted X-rays to a resolution of 1.60 Å. The crystals were determined to belong to the orthorhombic space group *I*222 (or $I2_12_12_1$), with unit-cell parameters a = 91.8, b = 99.6, c = 131.1 Å.

The asymmetric unit volume provides space for only one subunit of the tetrameric HpaB molecule, giving a Matthews coefficient V_M (Matthews, 1968) of 2.8 Å^3 Da^{-1}. This indicates that the space group may be *I*222, because *I*222 has 222 point-group symmetry which can generate the tetrahedral tetramer by crystallographic symmetry whereas $I2_12_12_1$ has no intersecting twofold axes and is not compatible with the formation of the biological tetramer, although the space group was determined on the basis of the Patterson map as described below. The solvent content was calculated to be 55.1%, which is within the range of values typically observed for protein crystals (Matthews, 1968). Crystallographic data and data-collection statistics are summarized in Table 1.

3.2. MAD data collection of the Pt-derivatized crystals

Crystals of the derivative protein were prepared by soaking the crystals in a reservoir solution containing 1 m*M* ammonium tetrachloroplatinate(II) [$(NH_4)_2PtCl_4$] for 1 d. The Pt-derivatized HpaB crystals diffracted X-rays to a resolution of 2.50 Å. Crystals were determined to belong to the orthorhombic space group *I*222 (or $I2_12_12_1$), with unit-cell parameters a = 92.3, b = 99.5, c = 131.3 Å. The X-ray absorption spectrum at the L_{III} edge of Pt was measured using one crystal. Incident wavelengths were selected with λ_{peak} = 1.0714 Å, λ_{edge} = 1.0714 Å and λ_{remote} = 0.9100 Å based on the X-ray absorption spectrum of each of the pairs in the trichromator for the Pt-derivatized crystal. The values of the peak and edge wavelengths agreed with each other by chance, since each monochromator contains an independent calibration error. Crystallographic data and statistics of the MAD data collection for the Pt-derivatized crystal are given in Table 1. The Pt-atom positions were obtained from a Patterson map calculated with the program *XtalView* (McRee, 1999) using the observed anomalous differences as coefficients. Harker sections of the anomalous difference Patterson map of the peak data set showed one large peak corresponding to a Pt atom in the asymmetric unit. The correct space group was determined to be *I*222 judging from the Patterson map. From this map, the position of the Pt atom was calculated to be (0.318, 0.155, 0.233) in Patterson space. The initial MAD phases were calculated using the program *SHARP* (de La Fortelle & Bricogne, 1997). Four additional minor Pt sites were found in the anomalous difference Fourier map. Density modification and phase extension to 1.6 Å was carried out with the program *RESOLVE* (Terwilliger, 2000), resulting in an auto-built model containing 395 out of 481 residues (figure of merit = 0.63). The quality of the electron-density map was sufficient to identify each amino-acid residue. Model building and refinement of the structure are in progress and structural details will be described elsewhere.

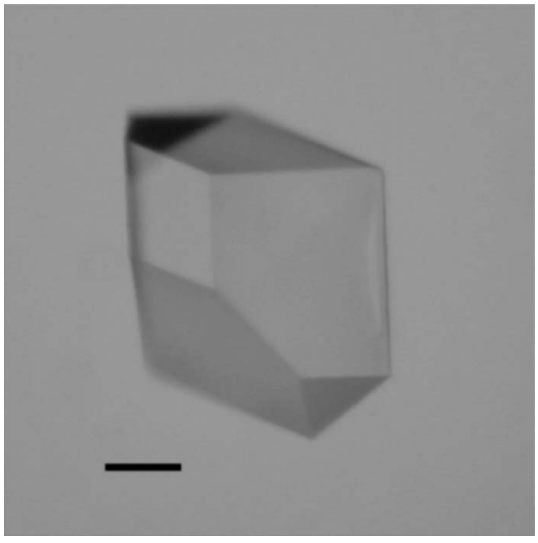

Figure 2
A crystal of HpaB obtained by the hanging-drop vapour-diffusion method. The bar corresponds to 0.1 mm.

Table 1
Data-collection and refinement statistics.

Values in parentheses are for the highest resolution shell.

	MAD data			
Data set	Remote	Peak	Edge	Native
Beamline and detector	BL45XU (SPring-8) and R-AXIS V			
Wavelength (Å)	0.9100	1.0714	1.0714	0.9000
Space group	*I*222			
Unit-cell parameters				
a (Å)	92.3			91.8
b (Å)	99.5			99.6
c (Å)	131.3			131.1
Resolution	40–2.50 (2.64–2.50)			50–1.60 (1.66–1.60)
No. of measurements	124253	116844	128139	375078
No. of unique reflections	21077	19966	21153	79180
Completeness	99.2 (98.7)	99.2 (97.5)	99.5 (99.2)	99.9 (100.0)
Redundancy	5.9 (4.9)	5.9 (4.9)	6.1 (5.3)	4.7 (3.6)
Average $I/\sigma(I)$	12.9 (5.6)	9.8 (3.8)	11.1 (5.2)	23.4 (8.3)
R_{merge}†	0.046 (0.130)	0.065 (0.191)	0.053 (0.138)	0.053 (0.349)
Phasing statistics (iso/ano)				
Phasing power				
Centric	—/—	0.465/—	0.696/—	
Acentric	—/1.140	0.404/1.175	0.619/0.975	
R_{cullis}				
Centric	—/—	0.815/—	0.747/—	
Acentric	—/0.795	0.829/0.783	0.783/0.835	

† $R_{merge} = \sum_{hkl}\sum_i |I_{hkl,i} - \langle I_{hkl}\rangle| / \sum_{hkl}\sum_i I_{hkl,i}$.

We would like to thank Dr Y. Kawano and Mr H. Nakajima of the Division of Bio-Crystallography Technology, RIKEN Harima Institute for their kind help in data collection. This work was performed under the 'Structurome' Project of RIKEN Harima Institute.

References

Ballou, D. P., Entsch, B. & Cole, L. J. (2005). *Biochem. Biophys. Res. Commun.* **338**, 590–598.
Berkel, W. J. H. van, Westphal, A. H., Eschrich, K., Eppink, M. & de Kok, A. (1992). *Eur. J. Biochem.* **210**, 411–419.
Cooper, R. A. & Skinner, M. A. (1980). *J. Bacteriol.* **143**, 302–306.
Entsch, B., Ballou, D. P. & Massey, V. (1975). *J. Biol. Chem.* **251**, 2550–2563.
Entsch, B., Cole, L. J. & Ballou, D. P. (2005). *Arch. Biochem. Biophys.* **433**, 297–311.
Galán, B., Díaz, E., Prieto, M. A. & García, J. L. (2000). *J. Bacteriol.* **182**, 627–636.
Galán, B., Kolb, A., García, J. L. & Prieto, M. A. (2001). *J. Biol. Chem.* **276**, 37060–37068.

Gisi, M. R. & Xun, L. (2003). *J. Bacteriol.* **185**, 2786–2792.
Kumasaka, T., Yamamoto, M., Moriyama, H. & Ueki, T. (2002). *Structure*, **10**, 1205–1210.
La Fortelle, E. de & Bricogne, G. (1997). *Methods Enzymol.* **276**, 472–494.
McRee, D. E. (1999). *J. Struct. Biol.* **125**, 156–165.
Maeda-Yorita, K. & Massey, V. (1993). *J. Biol. Chem.* **268**, 4134–4144.
Matthews, B. W. (1968). *J. Mol. Biol.* **33**, 491–497.
Otwinowski, Z. & Minor, W. (1997). *Methods Enzymol.* **276**, 307–326.
Prieto, M. A., Díza, E. & García, J. L. (1996). *J. Bacteriol.* **178**, 111–120.
Prieto, M. A. & García, J. L. (1994). *J. Biol. Chem.* **269**, 22823–22829.
Sucharitakul, J., Chaiyen, P., Entsch, B. & Ballou, D. P. (2006). *J. Biol. Chem.* **281**, 17044–17053.
Terwilliger, T. C. (2000). *Acta Cryst.* D**56**, 965–972.
Valton, J., Fontecave, M., Douki, T., Kendrew, S. G. & Nivière, V. (2006). *J. Biol. Chem.* **281**, 27–35.
Xun, L. & Sandvik, E. R. (2000). *Appl. Environ. Microbiol.* **66**, 481–486.